PROCEEDINGS OF SCIENCE

Novel description of $P_c(4312)^+$, $P_c(4380)^+$, and $P_c(4457)^+$ with double triangle cusps

Satoshi X. Nakamura*

University of Science and Technology of China,
Hefei 230026, People's Republic of China
State Key Laboratory of Particle Detection and Electronics (IHEP-USTC),
Hefei 230036, People's Republic of China

E-mail: satoshi@ustc.edu.cn

We propose a novel scenario for the peak structures, usually interpreted as hidden charm pentaquark (P_c) contributions, in the LHCb's $\Lambda_b^0 \to J/\psi p K^-$ data. The key idea is to utilize leading or lower-order singularities from double triangle mechanisms. The singularities cause anomalous threshold cusps, which are significantly more singular than the ordinary ones, at the $\Sigma_c^{(*)}\bar{D}^{(*)}$ threshold. We demonstrate that the double triangle amplitudes interfere with other common mechanisms to create peak structure that fit well the $P_c(4312)^+$, $P_c(4380)^+$, and $P_c(4457)^+$ peaks in the data. This picture is completely different from commonly used ones such as hadron molecules and compact pentaquarks. Meanwhile, $P_c(4440)^+$ is included in the proposed model as a resonance with width and strength significantly smaller than previously estimated. The proposed model can (partly) explain the current data for other processes where P_c^+ signals are expected such as: no P_c^+ signals in the GlueX J/ψ photoproduction data; a possible signal only from $P_c(4440)^+$ in the LHCb's $\Lambda_b^0 \to J/\psi p \pi^-$ data.

**** 10th International Workshop on Charm Physics (CHARM2020), ****
**** 31 May - 4 June, 2021 ****
**** Mexico City, Mexico - Online ****

*Speaker

PoS(CHARM2020)029

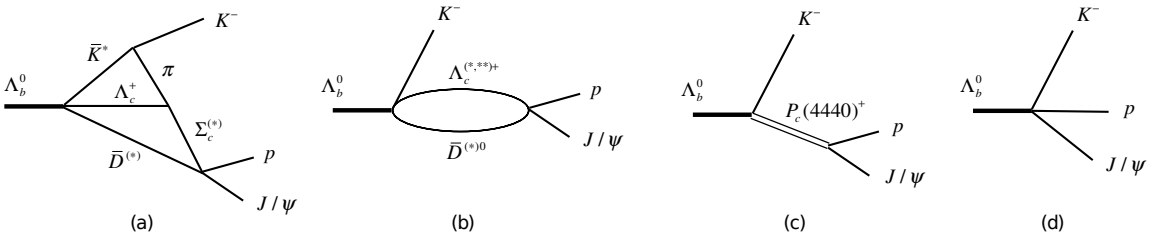

Figure 1: $\Lambda_b^0 \to J/\psi p K^-$ diagrams: (a) double triangle; (b) one-loop; (c) $P_c(4440)^+$-excitation; (d) direct decay. Figures taken from Ref. [4]. Copyright (2021) APS.

1. Introduction

The recent LHCb data on $\Lambda_b^0 \to J/\psi p K^-$ revealed three resonance(like) structures [1]. The peaks are considered to be contributions from pentaquark states called $P_c(4312)^+$, $P_c(4440)^+$, and $P_c(4457)^+$. Because the P_c^+ masses are slightly below the $\Sigma_c(2455)\bar{D}^{(*)}$ thresholds [1], one would be tempted to interpret P_c^+'s as $\Sigma_c(2455)\bar{D}^{(*)}$ molecules (bound states). Still, a compact pentaquark interpretation is also possible. P_c^+'s are expected to appear also in different processes. The J/ψ photoproduction off a nucleon seems a promising candidate. However, the GlueX experiment found no evidence [3]. This may indicate either that a photon couple weakly with the P_c^+ states, or that the P_c^+ peaks in $\Lambda_b^0 \to J/\psi p K^-$ are due to kinematical effects and do not appear in the photoproduction.

In this work [4], we identify double triangle (DT) diagrams [Fig. 1(a)] some of which are kinematically allowed to occur at the classical level. Thus, the diagrams have either the leading or lower-order kinematical singularities [5]. The double triangle singularities (DTS) cause anomalous threshold cusps. We show that these cusps are more singular than the ordinary threshold cusp. Therefore, the DTS may be exploited to interpret resonancelike structure. We demonstrate that the DT amplitudes interfere with other common mechanisms of Figs. 1(b) and 1(d) to reproduce the $P_c(4312)^+$, $P_c(4380)^+$, and $P_c(4457)^+$ peak structures in the LHCb data. Only one resonance is required to describe the $P_c(4440)^+$ peak. We find that $P_c(4440)^+$ from our analysis has width and strength significantly smaller than the LHCb's result. This new interpretation of the P_c signals is also (partly) consistent with other data such as the J/ψ photoproduction and $\Lambda_b^0 \to J/\psi p \pi^-$ data [6] that seem to show only a $P_c(4440)^+$ signal.

2. Model

We consider mechanisms for $\Lambda_b^0 \to J/\psi p K^-$ diagrammatically shown in Fig. 1. For loop diagrams [Fig. 1(a,b)], the initial weak decays of $\Lambda_b^0 \to \Lambda_c^{(*,**)+}\bar{D}^{(*)}\bar{K}^{(*)}$ are assumed to be induced by color-favored quark mechanisms. The $P_c(4440)^+$ amplitude [Fig. 1(c)] is given in the Breit-Wigner form. In each partial wave, a direct decay mechanism [Fig. 1(d)] is included. We consider $J^P = 1/2^-$, $3/2^-$, $1/2^+$, and $3/2^+$ partial waves; J^P denotes the spin-parity of $J/\psi p$. Amplitude formulas can be found in Ref. [4]. The $Y_c\bar{D}^{(*)}$ pairs in the DT and one-loop diagrams

[1] We follow the hadron name notation of Ref. [2]. In addition, we often denote $\Sigma_c(2455)^{+(++)}$, $\Sigma_c(2520)^{+(++)}$, $\Lambda_c(2595)^+$, and $\Lambda_c(2625)^+$ by Σ_c, Σ_c^*, Λ_c^*, and Λ_c^{**}, respectively. $\Lambda_c^{(*,**)}$ and $\Sigma_c^{(*)}$ are also collectively denoted by Y_c. We often suppress charge indices. We also denote a baryon (B) meson (M) pair with a spin-parity J^P by $BM(J^P)$.

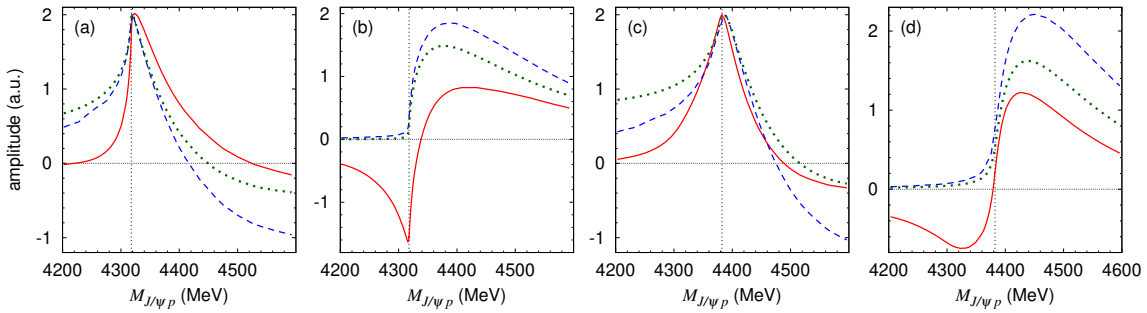

Figure 2: Double triangle amplitudes. (a) [(b)] The red solid curve shows the real [imaginary] part of the double triangle amplitude of Fig. 1(a) with $\Sigma_c^{(*)}\bar{D}^{(*)} = \Sigma_c^+\bar{D}^0$; $\Sigma_c^{(*)}\bar{D}^{(*)} \to J/\psi p$ is perturbatively considered. By using $m_{\Lambda_c^+} = 3$ GeV, they reduce to the blue dashed curves. The $\Sigma_c^+\bar{D}^0$ one-loop amplitude is shown by the green dotted curves. All the amplitudes are normalized so that the real parts have the same peak height. The dotted vertical lines indicate the $\Sigma_c^+\bar{D}^0$ thresholds. (c) [(d)] The amplitudes shown are obtained from those in (a) [(b)] by replacing Σ_c^+ with Σ_c^{*+}. Figures taken from Ref. [4]. Copyright (2021) APS.

are expected to be strongly interacting. We describe it with a single-channel contact interaction model, and then combine it with a perturbative transition to $J/\psi p$. We assume to absorb other possible coupled-channel effects in complex couplings fitted to the data.

3. Results

3.1 Singular behavior of double triangle amplitudes

The DT amplitude including $\Sigma_c^+\bar{D}^0$ $(1/2^-)$ is shown by the red solid curves in Fig. 2(a,b). The amplitude is singular near the $\Sigma_c^+\bar{D}^0$ threshold because it has the leading singularity. A $\Sigma_c^+\bar{D}^0$ one-loop amplitude, causing an ordinary threshold cusp, is also shown by the green dotted curves. The DT leading singularity creates a more singular cusp. By setting the Λ_c^+ mass in the DT amplitude at a hypothetically heavy value (3 GeV), the DT amplitude has only the $\Sigma_c^+\bar{D}^0$ threshold singularity. This is confirmed by the blue dashed curves shown in the figure. Similarly, we plot in Fig. 2(c,d) amplitudes obtained from those in Fig. 2(a,b) by replacing Σ_c^+ with Σ_c^{*+}. This DT amplitude with $\Sigma_c^{*+}\bar{D}^0$ has the lower-order singularity and, thus, it is less singular than the leadingly singular DT amplitude with $\Sigma_c^+\bar{D}^0$. Still, both are more singular than the ordinary threshold cusp.

How is a P_c peak created from a DT amplitude ? The DT amplitude including $\Sigma_c\bar{D}$ alone gives the $M_{J/\psi p}$ distribution shown by the blue dotted curve in Fig. 3. A peak in the spectrum is located at the $\Sigma_c\bar{D}$ threshold, as expected from Fig. 2. This peak position does not agree with $P_c(4312)$. By including the direct decay amplitude coherently, we obtain the green dashed curve with a peak slightly below the threshold. By further including the $\Lambda_c^+\bar{D}^{*0}$ one-loop amplitude, the red solid curve is obtained; now the peak position agrees with $P_c(4312)$.

3.2 Analyzing the LHCb data

We consider in our $\Lambda_b^0 \to J/\psi p K^-$ model: (i) DT mechanisms with $\Sigma_c(2455)\bar{D}$ $(1/2^-)$, $\Sigma_c(2520)\bar{D}$ $(3/2^-)$, $\Sigma_c(2455)\bar{D}^*$ $(1/2^-)$, $\Sigma_c(2455)\bar{D}^*$ $(3/2^-)$, $\Sigma_c(2520)\bar{D}^*$ $(1/2^-)$, and $\Sigma_c(2520)\bar{D}^*$ $(3/2^-)$;

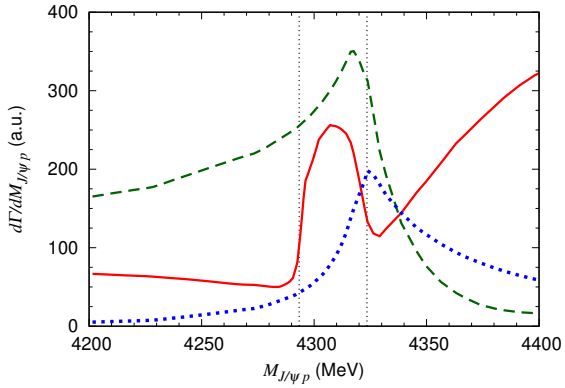

Figure 3: Formation of the $P_c(4312)^+$ peak from interference of different amplitudes. The blue dotted curve is the differential decay width ($d\Gamma/dM_{J/\psi p}$) solely from the double triangle amplitude including the $\Sigma_c\bar{D}$ pair. By adding a direct decay amplitude coherently, the green dashed curve is obtained. The red solid curve is obtained by further adding the $\Lambda_c^+\bar{D}^{*0}$ one-loop diagram. $Y_c\bar{D}^{(*)} \to J/\psi p$ is perturbatively considered. The dotted vertical lines indicate thresholds for, from left to right, $\Lambda_c^+\bar{D}^{*0}$ and $\Sigma_c(2455)^{++}D^-$, respectively.

(ii) one-loop mechanisms with $\Lambda_c^+\bar{D}^{*0}\,(1/2^-)$, $\Lambda_c(2595)^+\bar{D}^0\,(1/2^+)$, and $\Lambda_c(2625)^+\bar{D}^0\,(3/2^+)$; (iii) $P_c(4440)^+$ mechanism; (iv) direct decay mechanisms. Fitting parameters come from each mechanism in the items (i)-(iii) with an adjustable complex overall factor; 2×10 parameters. Four parameters from direct decay mechanisms (iv) each of which has a real coupling. Two parameters from the $P_c(4440)^+$ mass and width. One parameter from a repulsive $\Lambda_c^+\bar{D}^{*0}$ interaction strength. Because the full amplitude has an arbitrariness of the overall absolute normalization, we have 26 parameters in total.

Each of $Y_c\bar{D}^{(*)}(J^P)$ interactions are examined if the fit prefers an attraction or repulsion. We found attractions for $\Sigma_c(2455)\bar{D}\,(1/2^-)$, $\Sigma_c(2520)\bar{D}\,(3/2^-)$, $\Sigma_c(2455)\bar{D}^*\,(1/2^-)$, $\Sigma_c(2455)\bar{D}^*\,(3/2^-)$, $\Lambda_c(2595)^+\bar{D}^0\,(1/2^+)$, $\Lambda_c(2625)^+\bar{D}^0\,(3/2^+)$, and repulsions for $\Sigma_c(2520)\bar{D}^*\,(1/2^-)$, $\Sigma_c(2520)\bar{D}^*\,(3/2^-)$, $\Lambda_c^+\bar{D}^{*0}\,(1/2^-)$. Then we use a fixed coupling for the attraction so that the scattering length is $a\sim 0.5$ fm [2] We fit the repulsive $\Lambda_c^+\bar{D}^{*0}\,(1/2^-)$ coupling to the data to keep a good fit quality; $a\sim -0.4$, -0.2, and -0.05 fm for $\Lambda\sim 0.8$, 1, and 1.5–2 GeV, respectively (Λ: common cutoff in the form factors). The same coupling strength is used for the other repulsive $Y_c\bar{D}^{(*)}(J^P)$ channels. Spectrum peak positions are not very sensitive to the a values since they are essentially determined by the kinematical effects. We use $\Lambda = 1$ GeV at each interaction vertex; the result does not significantly depend on the cutoff value. An exception is applied to the direct decay amplitudes for which different cutoffs on $p_{\bar{K}}$ are used so that their $M_{J/\psi p}$ distribution is similar to the phase-space shape.

We compare the calculation, after smearing with the experimental resolution, with the LHCb data [1] in Fig. 4(a). The data are well fitted by our full model shown by the red solid curve. The considered mechanisms cause the kinematical effects to describe well the $P_c(4312)^+$, $P_c(4380)^+$, and $P_c(4457)^+$ peak structures. We utilized a pole ($J^P = 3/2^-$ in the figure) to fit only the $P_c(4440)^+$ peak. We varied the cutoff over $\Lambda = 0.8$–2 GeV and change J^P for $P_c(4440)^+$ over

[2]The scattering length (a) is related to the phase shift (δ) by $p\cot\delta = 1/a + O(p^2)$.

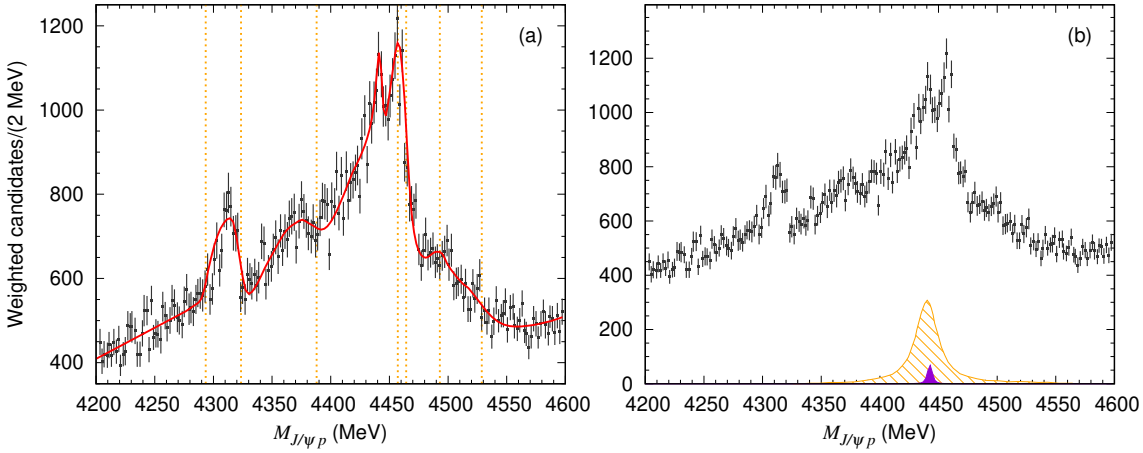

Figure 4: (a) Comparison with the LHCb data ($\cos\theta_{P_c}$-weighted samples) [1] for $J/\psi p$ invariant mass ($M_{J/\psi p}$) distribution of $\Lambda_b^0 \to J/\psi p K^-$. The red solid curve is from our model. The dotted vertical lines indicate thresholds for, from left to right, $\Lambda_c^+ \bar{D}^{*0}$, $\Sigma_c(2455)^{++} D^-$, $\Sigma_c(2520)^{++} D^-$, $\Lambda_c(2595)^+ \bar{D}^0$, $\Sigma_c(2455)^{++} D^{*-}$, $\Lambda_c(2625)^+ \bar{D}^0$, and $\Sigma_c(2520)^{++} D^{*-}$, respectively. (b) $P_c(4440)^+$ contribution. The orange striped peak is the $P_c(4440)^+$ contribution from the LHCb analysis. The solid violet peak is the $P_c(4440)^+(3/2^-)$ contribution from our model; the interference excluded. Figure is (partly) taken from Ref. [4]. Copyright (2021) APS.

$J^P = 1/2^\pm$ and $3/2^\pm$; the quality of the fit does not change significantly.

In Fig. 4(b), we show the $P_c(4440)^+(3/2^-)$ contribution from our analysis by the violet solid peak; an interference contribution is excluded. This contribution is described by the Breit-Wigner mass and width of 4443.1±1.4 MeV and 2.7±2.4 MeV, respectively. These values can be compared with those from the LHCb analysis [1], $4440.3 \pm 1.3^{+4.1}_{-4.7}$ MeV and $20.6 \pm 4.9^{+8.7}_{-10.1}$ MeV, shown by the orange striped peak in Fig. 4(b). The width from our analysis is significantly narrower. Also, our $P_c(4440)^+$ contribution is smaller by a factor of ∼22 than the LHCb's estimate: $\mathcal{R} \equiv \mathcal{B}(\Lambda_b^0 \to P_c^+ K^-)\mathcal{B}(P_c^+ \to J/\psi p)/\mathcal{B}(\Lambda_b^0 \to J/\psi p K^-) = 1.11 \pm 0.33^{+0.22}_{-0.10}$ %. This large difference comes from different fitting strategies. The LHCb used incoherent $P_c(4440)^+$ and $P_c(4457)^+$ contributions to fit the large structure at $M_{J/\psi p} \sim 4450$ MeV. On the other hand, we utilized the kinematical effects to describe a large portion of the structure, and fit the remaining small spike with the $P_c(4440)^+$ and its interference.

The LHCb found an evidence for P_c^+ also in $\Lambda_b^0 \to J/\psi p \pi^-$. In their $M_{J/\psi p}$ distribution [Fig. 3(b) of [6]], the $M_{J/\psi p}$ bin of $P_c(4440)^+$ seems to be enhanced. However, no visible enhancement is found for the other P_c^+'s. This observation is actually consistent with our model's expectation because $\Lambda_b^0 \to J/\psi p \pi^-$ does not have a relevant DT mechanism but can share the $P_c(4440)^+$ excitation mechanism. However, the $\Lambda_b^0 \to J/\psi p \pi^-$ data may conflict with some other P_c^+ models. The P_c^+ signals in $\Lambda_b^0 \to J/\psi p \pi^-$ are still inconclusive due to the limited quality of the data. Forthcoming LHCb Run II data on $\Lambda_b^0 \to J/\psi p \pi^-$ might seriously challenge the models.

4. Summary

We developed a model for $\Lambda_b^0 \to J/\psi p K^-$ and analyzed the $M_{J/\psi p}$ distribution data from the LHCb. The double triangle cusps and their interference with the common mechanisms describe well the P_c^+ structures. $P_c(4440)^+$ is the only resonance in our analysis, and its width and strength are much smaller than those from the LHCb analysis. This interpretation of the P_c^+ peaks is completely different from the commonly used hadron molecules and compact pentaquarks. The DT cusps can appear in different processes and thus they should now be an option to interpret resonancelike structures near thresholds.

Acknowledgments

This work is in part supported by National Natural Science Foundation of China (NSFC) under contracts U2032103 and 11625523, and also by National Key Research and Development Program of China under Contracts 2020YFA0406400.

References

[1] R. Aaij et al. (LHCb Collaboration), *Observation of a Narrow Pentaquark State, $P_c(4312)^+$, and of the Two-Peak Structure of the $P_c(4450)^+$*, *Phys. Rev. Lett.* **122** (2019) 222001 [1904.03947 [hep-ex]].

[2] P.A. Zyla et al. (Particle Data Group), *The Review of Particle Physics*, *Prog. Theor. Exp. Phys.* **2020** (2020) 083C01.

[3] A. Ali et al. (GlueX Collaboration), *First measurement of near-threshold J/ψ exclusive photoproduction off the proton*, *Phys. Rev. Lett.* **123** (2019) 072001 [1905.10811 [nucl-ex]].

[4] S.X. Nakamura, *$P_c(4312)^+$, $P_c(4380)^+$, and $P_c(4457)^+$ as double triangle cusps*, *Phys. Rev. D* **103** (2021) L111503 [2103.06817 [hep-ph]].

[5] R. J. Eden, P. V. Landshoff, D. I. Olive and J. C. Polkinghorne, *The Analytic S-Matrix*, Cambridge University Press, Cambridge, England, 1966.

[6] R. Aaij et al. (LHCb Collaboration), *Evidence for exotic hadron contributions to $\Lambda_b^0 \to J/\psi p\pi^-$ decays*, *Phys. Rev. Lett.* **117** (2016) 082003 [1606.06999 [hep-ex]].